

Transmembrane transport via integral proteins

8-1. Introduction: Passive carrier-mediated transmembrane transport

8-1.1. Evidence for permeation by facilitating transporters

8-1.2. Unidirectional fluxes

8-1.3. Kinetics of facilitated transport

8-1.4. Unidirectional flux with zero transconcentration

8-1.5. Application to tracer experiments on capillary permeability

8-1.6. Unidirectional flux with finite trans concentration

8-2. Tracer transients with saturable transport

8-2.1. Additional topics for study

8-3. Problems

8-4. References

8-1. Introduction: Passive carrier-mediated transmembrane transport

Black lipid membranes, phospholipid bilayers containing no protein, are virtually impermeable to hydrophilic solutes, even water itself. The generality is that all hydrophilic solutes require the presence of some special transmembrane molecule, usually a protein, to traverse the bilayer.

Some integral membrane proteins serve simply as conduits for specific solutes. For example, aquaporin transports water selectively but passively, and a potassium-selective channel protein serves the time-independent I_K current (Winslow et al., 1999) whose conductances seem purely passive, independent of concentration. Yet they are selective!

The ionic channels with time- and voltage-dependent kinetics discussed in Chapter 7 are passive, even while being selective: the currents are driven solely by the electrochemical gradients for the ion. Such channels are not energetically coupled, and when open they allow the passage of many ions, often thousands per millisecond. Their selectivity is not by any means total, but is limited to a few similarly charged and sized ions or ionized solutes. These are not considered to be “transporters”, but rather are channels, because when they are open the rate of transfer depends on the driving forces across the membrane and not on the rate of change of conformational state of the protein. In contrast, carriers or transporters selectively bind substrates at a surface site and carry the substrate across the membrane at a rate depending on the state of the carrier rather than on the driving force for substrate. Thus the transport rate depends on the number of carrier proteins per unit surface area of membrane, the fraction of sites filled, and the rate of conformational state to carry the active site from one side of the membrane to the other.

How does one distinguish carrier-mediated transport from that due to channels or other passive leaks? A somewhat vague rule is that whenever a solute traverses the membrane faster than “expected”, it is likely that a transporter molecule can be found to explain the flux. The “expected” permeability is that estimated by comparison with other molecules of similar water-lipid solubilities and molecular size and hydrophobicity (Tanford, 1961; Stein, 1986).

8-1.1. Evidence for permeation by facilitating transporters

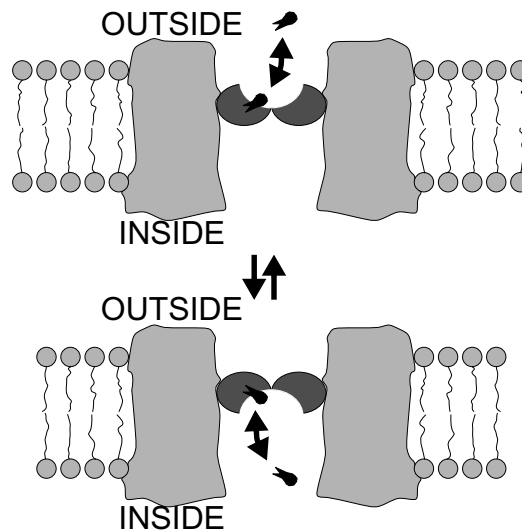


Figure 8-1: A membrane transporter selectively binds a solute to a high-affinity site, then there is a conformational change to flip the site (and the bound solute) to face the opposite side of the membrane allowing release of the solute on the other side of the membrane.

By facilitated transport, as in Fig. 8-1, one means transport across a membrane under the normally existent electrochemical gradient, without energetic coupling and without the need for energy supplied by another solute moving down its electrochemical gradient. There is no requirement for energy supplied by ATP, which is termed “active transport”. There is no requirement for coupling to the dissipation of an energy potential for another solute, which is termed “coupled transport”, facilitated by an exchanger, such as the sodium-calcium exchanger. Passive facilitated transport was termed ‘facilitated diffusion’ when it was first identified and characterized. This early era is reviewed in the pioneering studies of Wilbrandt and Rosenberg (1961) and the texts by W.D. Stein (1967, 1986).

Suspect the use of a special transporter when:

1. Fluxes rise to a plateau, a maximum, as substrate concentrations are raised, rather than following Fick’s first law. In other words, the apparent conductivity diminishes with increasing concentration. This is “*saturation kinetics*”, and is a strong inference, although it is dependent on parallel evidence in the experiment that the fluxes of other unrelated solutes are unchanged by the concentrations of the particular substrate.
2. Transport is inhibited by molecules of analogous structure. This is *competition*, and is also a strong inference.
3. There is inhibition of tracer-labeled substrate transfer by the presence of nontracer mother substrate (that is, *self-competition* by the unlabeled substrate). This observation is almost sure evidence.
4. There is facilitation of the unidirectional tracer-labeled substrate flux by the flux of a molecule of similar structure down its electrochemical gradient in the opposite direction.

This is a special case, *exchange transport facilitation*, that virtually guarantees the existence of a transporter.

5. There is inhibition of flux by unlike substances but which are specific to the transport of specific permeant. These *transport blockers*, like enzyme blockers, are usually poisons which bind tightly to the transporter and stop its action. (These inhibitors fall into the classes of competitive inhibitors, ones that can be displaced from the active site by high substrate concentrations, and non-competitive inhibitors, ones which bind elsewhere on the transporter molecule but induce conformational changes that preclude or reduce substrate binding to the transporter or the conformational change effecting the translocation across the membrane.) The inhibition must be specific, not affecting the membrane itself or the fluxes of unrelated solutes.
6. *There are inexplicably high fluxes*, higher than expected from the physicochemical characteristics of the substrate. This is not a very strongly inferential point, but does illustrate why transporters exist for so many solutes: normal rates of penetration are too slow to maintain the metabolic needs of the cell.

8-1.2. Unidirectional fluxes

Unidirectional versus net fluxes: The measurement of rates of changes in chemical concentrations in one or both of two mixing chambers separated by a membrane gives a measure of net flux across the membrane, as in Eq. 8-1. The dependence of the rate on the concentration is expressed by the form $k(C)$:

$$\frac{dC}{dt} = -k(C) \cdot C \quad (8-1)$$

While data obtained in chemical flux studies can be interpreted very often to yield estimates of unidirectional rates, e.g. by model fitting of the data, it is often most efficient to use tracers to measure the unidirectional fluxes. When there is no chemical gradient across the membrane, the rate of tracer flux indicates the unidirectional flux under the specific conditions, i.e. provides the measure of $k(C)$ at the ambient levels of C . This is important because when transport is carrier-mediated the tracer flux is controlled by the sum of the concentrations of the tracer, C' , and the mother substance:

$$\frac{dC'}{dt} = -k(C + C') \cdot C'. \quad (8-2)$$

However by the definition that a tracer molecule is chemically identical to the mother solute molecule, and that the tracer concentration is many orders of magnitude smaller than that of the mother solute, and therefore has negligible influence itself on the $k(C)$, this equation reduces to:

$$\frac{dC'}{dt} = -k(C) \cdot C', \quad (8-3)$$

and since $k(C)$ is a constant that is not changed by changes in tracer concentration, the system is linear and first order so far as tracer flux is concerned.

This generality holds true even when many solutes affect the rate constant, so that by changing the concentrations of each of the influencing chemicals in a series of tracer flux measurements one can distinguish the varied effects, inhibitions, enhancements, competition, etc., exploring the variant conditions:

$$\frac{dC_1'}{dt} = -k(C_1, C_2, C_3, \dots, C_{n-1}, C_n) \cdot C', \quad (8-4)$$

where the subscripted C's are the concentrations of all the various solutes interaction with the transporter. This expression holds true in this simple form only when all the C's are in steady state. In this state $k(C)$ remains a constant and the tracer system equations are first order.

Unidirectional fluxes are measurable under two sets of conditions: (1) fluxes are measurable from tracer measurements when there is a source of tracer on one side of the membrane only, and (2) fluxes are measurable from measurements of nontracer mother substrate when there is no substrate on one side of the membrane. The advantage of using tracer methods is that one can get a measure of unidirectional flux even if there is mother substance on both sides, and one can therefore explore a wide variety of conditions. By Fick's first law the exchange of substrate is

$$J_{S_{1,2}} = P(C_1 - C_2), \quad (8-5)$$

where J_S is flux per unit area of membrane, $\text{mol s}^{-1} \text{cm}^{-2}$, P is permeability, cm s^{-1} , and C_1 and C_2 are the concentrations, mmol cm^{-3} , on the cis (side 1) and trans (side 2) sides of the membrane. For the unidirectional flux, C_2 must be 0. For this reason, the experimental method is [to what](#) are called "initial velocity studies": the tracer, or the mother substrate, is placed on side 1 and the concentrations on side 2 are obtained at a succession of times. At early times the concentration on side 2 is so low that the backflux, P times C_2 , is negligibly low; the slope, dC_2/dt , can be determined as a best straight line for some time before the influence of the backflux diminishes the slope.

The strategy of examining the initial velocities before C_2 rises works well for studies of transporter fluxes. The initial slopes, as are found in a sequence of experiments at different mother substance concentrations, Fig. 8-2, upper, and the pseudo-steady state slopes plotted versus $C_1(t=0)$, as in the lower panel. The result, Fig. 8-2 lower, is that the flux -to-substrate concentration relationship fits the relationship:

$$J_S = \frac{V_{\max} S}{K_m + S}, \quad (8-6)$$

where V_{\max} is a maximum flux at high substrate concentrations, S , and the K_m is an apparent affinity of substrate for transporter and is the substrate concentration at which the flux is half-maximal. The curve has the shape of a single-site binding relationship or Langmuir adsorption. This is an excellent generality; higher-order binding to a transporter is certainly possible but is uncommon. In the next sections the basis for the expression is explained.

[\[Careful examination of the "straight lines" of the upper panel of Fig. 8-2 shows that there is an initial curvature at early times before the line straightens out.](#) Each of the lines can be seen to have a positive intercept on the time axis, e.g. by placing a ruler along any of them between 0.4

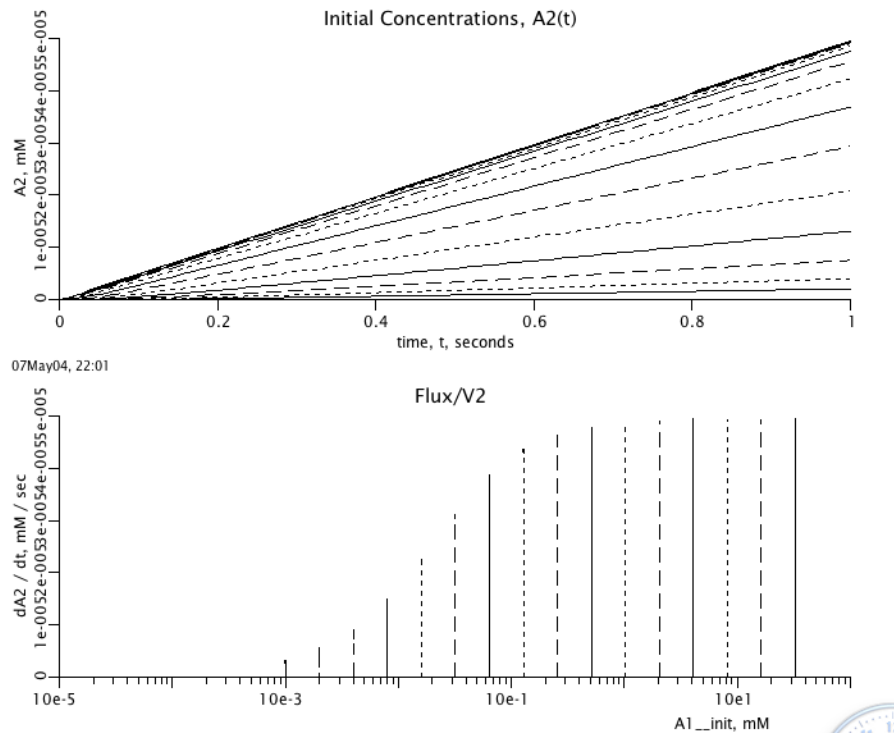


Figure 8-2: Initial transport velocities. A solute with concentration C_1 in volume V_1 permeates the membrane. *Upper panel:* Observations of the time course of concentration C_2 in volume V_2 are made at very early times such that $C_1 \ll C_2$ and C_1 is not measurably depleted by the loss due to the permeation. This is done over a wide range of starting conditions, $C_1(t=0)$ indicated by the vertical lines in the lower panel. *Lower panel:* The fluxes, $V_2 dC_2/dt$, are plotted as a function of $C_1(t=0)$; each starts with a rate near zero and rises to a steady-state maximum within the first second. At high concentrations the steady-state fluxes (tops of the vertical lines) approach a maximum asymptotically. That the levels of $C_1(t=0)$ were pushed high enough to reach V_{\max} , the maximum velocity of transport, is shown by the fact that at high levels the slopes, dC_2/dt in the left panel, are all the same.

and 1.0 seconds; the delay is membrane capacitance due to solute binding to transporter. This is analogous to the delay that was seen in diffusion studies with thick membranes and which produced the intercept L in the Barrer timelag analysis described in Chapter 5 (Barrer, 1953).] The apparent K_d is greater than the actual K_d , a result of a slow binding rate to be elucidated below..

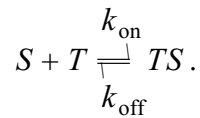
8-1.3. Kinetics of facilitated transport

The process of assisted, or facilitated, permeation of a membrane occurs via binding to specialized sites on proteins or other membrane-spanning molecules). The term “facilitated” generally implies “saturable transport”. The integral protein, the “transporter”:

- has finite abundance, having a total concentration T_T , moles/cm³ in the membrane;

- functions to allow the binding site to face either side of the membrane by undergoing a conformational change of one sort or another, for example, channel-narrowing behind a transported molecule (Klingenberg, 1981); [Fig. 8-1.]
- has highest affinity for substrates molecules of a select type;

The description of the simplest form of transporter begins with a binding reaction following first-order kinetics, solute S binding to transporter T . This gives a second-order overall reaction when reactions at both surfaces of the membrane are included:



The kinetics for association and dissociation, assuming that subsequent reactions for translocation are relatively very slow, are written:

$$\frac{dTS}{dt} = k_{\text{on}} \cdot T \cdot S - k_{\text{off}} \cdot TS \quad (8-7a)$$

$$\frac{dS}{dt} = -k_{\text{on}} \cdot T \cdot S + k_{\text{off}} \cdot TS, \quad (8-7b)$$

$$\frac{dT}{dt} = -\frac{dTS}{dt}, \quad (8-7c)$$

where T , TS and S are concentrations of uncomplexed or free transporter, transporter-substrate complex and free substrate, mol cm³. When the on and off rates are fast compared to the rate of transporter conformational change (flipping), then there is a local equilibrium at each surface:

$$k_{\text{eq}} = \frac{k_{\text{off}}}{k_{\text{on}}} = \frac{T \cdot S}{TS}. \quad (8-8)$$

When the equilibrium constant is the same on both sides of the membrane, this simplifies the equations for transport, as in Fig. 8-3. It also introduces a systematic error if it is not exactly true, a point discussed below.

Now consider the two-sided membrane, inside i and outside o , lying between two stirred media: *six species* (three concentrations on each side of the membrane) and four rate constants (for association and dissociation on each side) are involved. Assuming equilibrium allows TS_i to be calculated algebraically from S_i and the total concentration of transporter on that side of the membrane, $T_i + TS_i$, such that the ratio in Eq. 8-8 is matched. While $T_i + TS_i$ may change from one moment to the next as S_i or S_o are changed, the total transporter in the membrane is conserved:

$$\begin{aligned} T_T &= \text{sum of concentration of all transporter forms} \\ T_T &= T_i + TS_i + T_o + TS_o. \end{aligned} \quad (8-9)$$

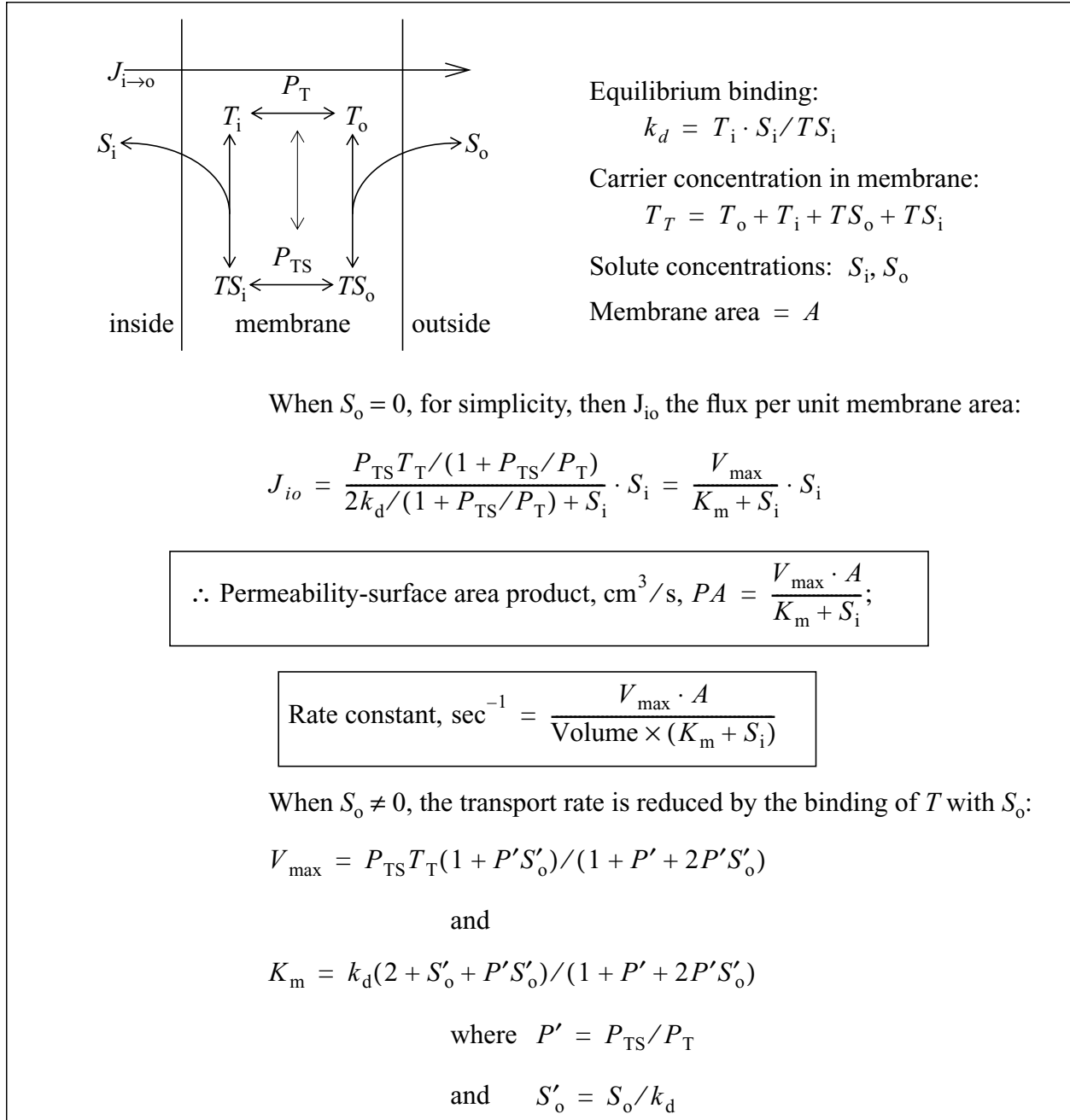


Figure 8-3: Transport via carrier facilitation. Summary of model for single-site binding, with local equilibration between solute, S , and transporter, T at the two surfaces. Two forms are given for J_{io} , one for when the solute concentration, S_o , on the trans (opposite) side of the membrane is zero, and a second, more complex form, when $S_o > 0$.

The unidirectional flux of solute-transporter complex per unit surface area from inside the cell to outside, $J_{TS_{io}}$, $\text{mol} \cdot \text{cm}^{-2} \text{s}^{-1}$, is

$$J_{TS_{io}} = P_{TS} \cdot TS_i, \quad (8-10)$$

and the net flux is

$$J_{\text{Net } TS_{io}} = P_{TS} \cdot (TS_i - TS_o). \quad (8-11)$$

The flux of total transporter $J_{T_{io}}$ (in forms T and TS) from inside the cell to outside is the sum for free and complexed transporter:

$$J_{T_{io}} = P_T T_i + P_{TS} \cdot TS_i,$$

and since $TS_i = T_i \cdot S_i/k_d$ from Eq. 8-8, and we define $S'_i = S_i/k_d$ and $S'_o = S_o/k_d$:

$$J_{T_{io}} = T_i(P_T + P_{TS} \cdot S'_i), \quad (8-12)$$

where the concentrations of S are normalized by dividing by the equilibrium dissociation constant k_{eq} , which is assumed here to be the same on both sides.

When the volumes of the solutions on the two sides of the membrane are large enough that transmembrane fluxes change the solution concentrations slowly **compared to shifts** in the distribution of the transporter with translocation (flips, conformational changes), then, moments after any redistribution a local steady state is reached, and **the** fluxes of transporter in the two directions must be equal and opposite:

$$J_{T_{io}} + J_{T_{oi}} = 0. \quad (8-13)$$

This is in effect assuming that dS_i/dt is much less than either dT_i/dt or dTS_i/dt occurring with association and dissociation of solute. **This simplifications implies that** $T_T \ll S$ and that $dS_i/dt \ll dT_i/dt$. This assumption was implicit in the pioneering work of Wilbrandt and Rosenberg, 1961, and Foster and Jacquez, 1975.

Rewriting Eq. 8-13 gives

$$T_i(P_T + P_{TS}S'_i) - T_o(P_T + P_{TS}S'_o) = 0, \quad (8-14)$$

$$T_i = \frac{(P_T + P_{TS}S'_o)}{(P_T + P_{TS}S'_i)} \cdot T_o = \frac{\gamma_o}{\gamma_i} \cdot T_o. \quad (8-15)$$

These γ 's have the same units as the P 's, i.e., permeability (cm s^{-1}) as defined in Eq. 8-15.

For transporter conservation, from Eq. 8-9,

$$T_T = T_i + TS_i + T_o + TS_o \quad (8-16a)$$

$$= T_i(1 + S'_i) + T_o(1 + S'_o) \quad (8-16b)$$

$$= T_i\delta_i + T_o\delta_o \quad (8-16c)$$

$$\text{and } T_i = \frac{T_T}{\delta_i} - T_o \frac{\delta_o}{\delta_i}. \quad (8-16d)$$

The δ 's defined in Eqs. 8-16a to 8-16d are scalars (dimensionless) that are governed by the solute concentrations and the equilibrium dissociation constants. Combining Eqs. 8-15 and 8-16a to 8-16d:

$$\frac{\gamma_o \cdot T_o}{\gamma_i} = T_i = \frac{T_T}{\delta_i} - T_o \cdot \frac{\delta_o}{\delta_i}, \quad (8-17a)$$

$$T_o = T_T \cdot \frac{\gamma_i}{\gamma_o \delta_i + \gamma_i \delta_o}, \quad (8-17b)$$

$$T_i = T_T \cdot \frac{\gamma_o}{\gamma_o \delta_i + \gamma_i \delta_o}, \quad (8-17c)$$

from which one calculates the unidirectional fluxes for the solute-transporter complex, which is the same as that for the solute (and assuming Eq. 8-8, $TS_i = T_i \cdot S_i/k_{eq} = T_i S'_i$):

$$J_{io} = P_{TS} \cdot TS_i = T_T \cdot \frac{\gamma_o}{\gamma_o \delta_i + \gamma_i \delta_o} \cdot (P_{TS} \cdot S'_i), \quad (8-18a)$$

$$J_{oi} = P_{TS} \cdot TS_o = T_T \cdot \frac{\gamma_i}{\gamma_o \delta_i + \gamma_i \delta_o} \cdot (P_{TS} \cdot S'_o) \quad . \quad (8-18b)$$

From Eq. 8-18a, the effective conductance P_{eff} for the unidirectional efflux, J_{io} , of solute is

$$P_{eff}(J_{io}) = \frac{T_T P_{TS} \cdot \gamma_o}{\gamma_o \delta_i + \gamma_i \delta_o}. \quad (8-19)$$

The net efflux per unit surface area is

$$J_{Netio} = J_{io} - J_{oi}. \quad (8-20)$$

8-1.4. Unidirectional flux with zero transconcentration

With $S_o = 0$ the expression for efflux simplifies since $\gamma_o \rightarrow P_T$ and $\delta_o \rightarrow 1$. Regrouping terms in Eq. 8-18a and using P' for P_{TS}/P_T :

$$J_{io} = \frac{T_T P_{TS} S'_i}{2 + S'_i(1 + P')} \quad (8-21a)$$

$$= \frac{T_T \cdot \frac{P_{TS}}{1+P'} \cdot S_i}{2k_{eq}/(1+P') + S_i} \quad (8-21b)$$

When $P_{TS} = P_T$, both forms of the carrier **having** equal likelihood to flip to the opposite side, then

$$J_{io} = \frac{\frac{1}{2}T_T \cdot P_{TS} \cdot S_i}{k_d + S_i} \quad (8-22)$$

This is the standard “Michaelis-Menten”-like first-order expression for an enzymatic reaction, now applied to carrier transport, using V_{\max} as the maximum transport rate and K_m as the “apparent Michaelis constant”, and where $K_m = K_d$ when the binding-unbinding is infinitely fast:

$$J_{io} = \frac{V_{\max} S_i}{K_m + S_i} \quad (8-23)$$

Thus for Eqs. 8-21a and 8-21b, we see that

$$V_{\max} = T_T \cdot P_{TS}/(1+P'), \quad (8-24a)$$

$$K_m = 2k_d/(1+P') \quad (8-24b)$$

Figure 8-4 provides some useful clues as to overall behavior.

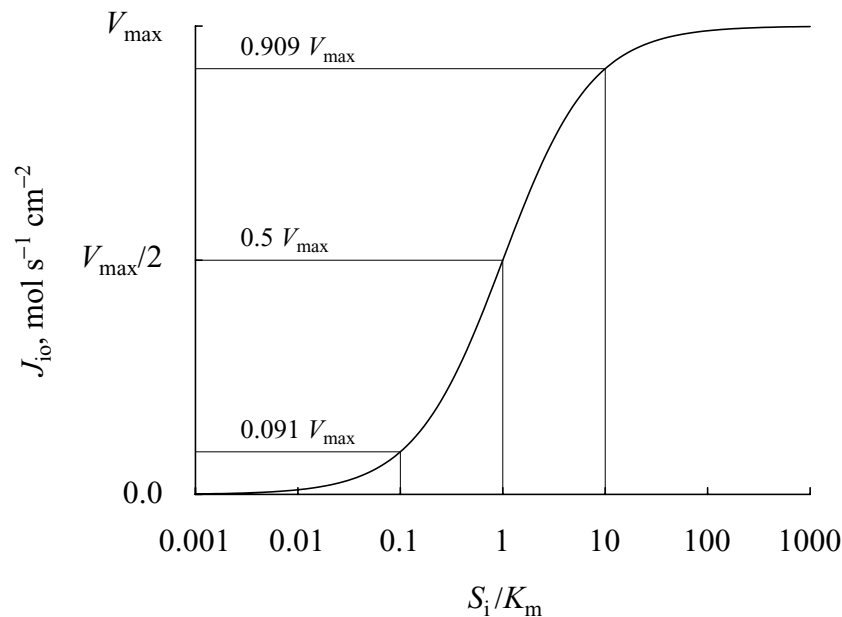


Figure 8-4: Saturation kinetics with a facilitating transporter.

1. When $S_i = K_m$, the flux is half-maximal: $J_{io} = V_{\max}/2$.

2. When $S_i = 10K_m$ and $100K_m$, then $J_{io} \approx 90.9\%$ and 99% of V_{max} .
3. When $S_i = 0.1K_m$ and $0.01K_m$, then $J_{io} \approx 9.1\%$ and 1% of V_{max} .
4. The slope $dJ_{io}/d(S_i/K_m)$ is $V_{max}/(1 + S')^2$. It is steepest at the inflection point $S_i = K_m$, where it is $V_{max}/4$.
5. At low substrate concentrations, $S_i \ll K_m$, the process is first order, $J_{io} = V_{max}/K_m$.
6. There are four unknown parameters in Eq. 8-24a and 8-24b. It is clear that the combination $T_T P_{TS}$ always appears as a product and these are therefore inseparable kinetically. Likewise $(1 + P')$ is always combined with another term.

Thus, raising the concentration S_i fills the binding sites and the transport efflux rises to a maximum when all the sites on the inside, side i, are occupied all the time.

The effective permeability for the solute is therefore a concentration-dependent value, as is shown in Fig. 8-5, and is

$$P_{eff} = \frac{T_T \cdot P_{TS}/(1 + P')}{2k_d/(1 + P') + S_i}. \quad (8-25)$$

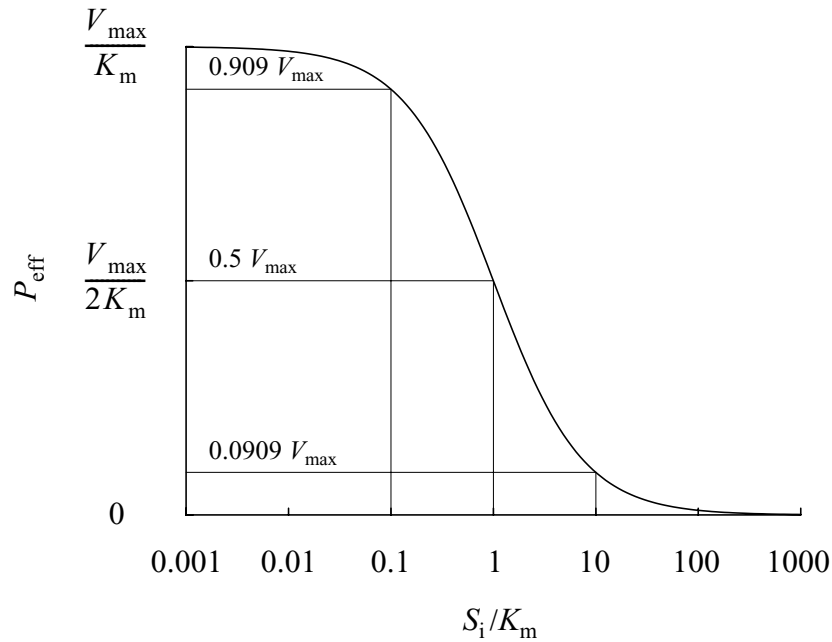


Figure 8-5: Effective permeability for unidirectional flux for a saturable transporter.

The case where $P_{TS} = P_T$, or $P' = 1$, is a common case since the solute molecule does not often influence the rate of conformational change.

$$J_{io} = \frac{T_T \frac{P_{TS}}{2} \cdot S_i}{k_d + S_i}, \quad (8-26a)$$

$$\text{where } V_{\max} = \frac{1}{2} T_T P_{TS} \quad (8-26b)$$

$$\text{and } K_m = k_d . \quad (8-26c)$$

This is now the standard Michaelis-Menten transporter expression; it explicitly identifies V_{\max} as the product of $T_T/2$ (since half of the transporter faces each side of the membrane) times the rate of conformational change, P_{TS} . The trans-concentration has no influence on J_{io} when $P_{TS} = P_T$ and affinity is the same on both sides, $k_{di} = k_{do}$. The effective P_{eff} , for the case when $P' = 1$, diminishes as S_i is increased (and is also diminished by increasing S_o):

$$P_{\text{eff}}(P' = 1) = \frac{V_{\max}}{K_m + S_i} = \frac{\frac{1}{2} T_T P_{TS}}{k_d + S_i} . \quad (8-27)$$

Note the similarity in the shape of PS in Fig. 8-5 to that of the volume of distribution for a solute-specific binding site as shown in Chapter 10, Fig. 10.5. The effective volume of distribution and the effective transporter PS diminish at higher substrate concentrations for the same reason—at higher S_i fewer binding sites are available.

At very low S_i where $S_i'(1 + P_{TS}) \ll 2$, the S_i in the denominator becomes negligible and Eqs. 8-21a and 8-21b reduce to

$$J_{io} = \frac{T_T \cdot P_{TS}}{2k_d} \cdot S_i . \quad (8-28)$$

This is now a *linear equation* with an apparent or effective permeability $P_{\text{eff}} = T_T \cdot P_{TS}/2k_d$ and is independent of S_i , so long as $S_i < 0.01 k_d$.

8-1.5. Transporter equations allowing for slow binding and release:

In the preceding section the reduction to the algebraic equations was based on the assumptions that: (1) the solute binding and unbinding reactions were fast compared with the translocation of the substrate-transporter complex, and (2) the transporter concentration is small compared with that of the substrate. When that is not the case there are then six molecular species to consider, namely the solute concentrations on the two sides of the membrane, and the two forms of the transporter, free and complexed with solute, on each side, as follows in Eqs. 8-29a to Eqs. 8-29g:

$$\frac{dS_1}{dt} = -k_{on1} \cdot T_1 \cdot S_1 + k_{off1} \cdot TS_1 , \quad (8-29a)$$

$$\frac{dT_1}{dt} = -k_{on1} \cdot T_1 \cdot S_1 + k_{off1} \cdot TS_1 - k_{T12} \cdot T_1 + k_{T21} \cdot T_2 \quad (8-29b)$$

$$\frac{dT S_1}{dt} = k_{on1} \cdot T_1 \cdot S_1 - k_{off1} \cdot T S_1 - k_{TS12} \cdot T S_1 + k_{TS21} \cdot T S_2 , \quad (8-29c)$$

$$\frac{dT S_2}{dt} = k_{on2} \cdot T_2 \cdot S_2 - k_{off2} \cdot T S_2 + k_{TS12} \cdot T S_1 - k_{TS21} \cdot T S_2 , \quad (8-29d)$$

$$\frac{dT_2}{dt} = -k_{on2} \cdot T_2 \cdot S_2 + k_{off2} \cdot T S_2 + k_{T12} \cdot T_1 - k_{T21} \cdot T_2 , \quad (8-29e)$$

$$\frac{dS_2}{dt} = -k_{on2} \cdot T_2 \cdot S_2 + k_{off2} \cdot T S_2 . \quad (8-29f)$$

with the constraint that

$$T_{tot} = T_1 + T_2 + T S_1 + T S_2 = \text{a constant} , \quad (8-29g)$$

so that the equation for T_2 can be replaced by $T_2 = T_{tot} - T S_1 - T_1 - T S_2$.

From the thermodynamic point of view there is another constraint that applies when the system is not coupled to an energy source, namely the Haldane constraints that apply to any reversible chemical reaction: For a passive transporter, the transport rate constants should satisfy the following:

$$\frac{k_{TS12} \cdot k_{T21} \cdot k_{on1} \cdot k_{off2}}{k_{TS21} \cdot k_{T12} \cdot k_{off1} \cdot k_{on2}} = 1 \quad (8-30)$$

These constraints ensure that the model runs to equilibrium at steady-state. If the ratio deviates from 1, the model will run to a steady-state net concentration gradient. This could be the case if the transporter is coupled to an energy source, which is not explicitly modeled here. A solution is provided in Fig. 8-6 for the system with the only substrate initially being A1.

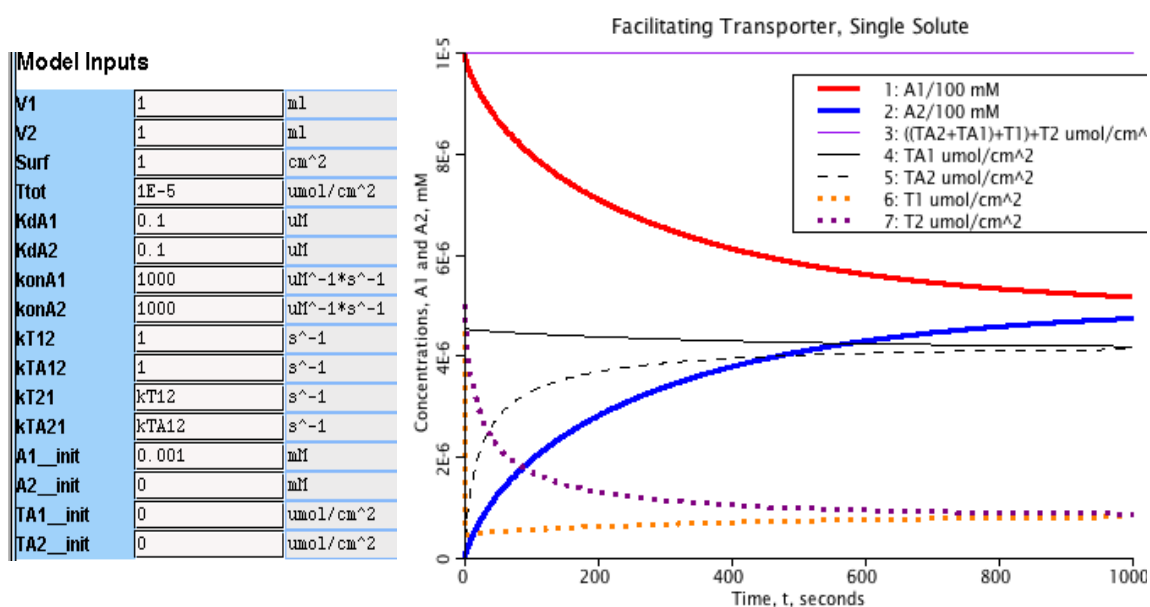


Figure 8-6: Transporter kinetics with finite rate of binding. Note that $A_1(t=0) = 1 \mu\text{M}$, only 10 times the k_{dA1} . A_1 equilibrates with A_2 at over 3000 seconds, but at a value less than $0.5 A_1(t=0)$, namely $0.496 A_1(t=0)$, because some A is attached to the transporter sites, 80% of which are occupied, as TA_1 and TA_2 . The sum of the 4 transporter forms is constant.

The code for a transporter that may bind with one of two competing substrates, A and B, is shown, with units, in Table 8-1. The results in Fig. 8-6 for the single solute may be reproduced by

Table 8-1: facT2, two solutes competing for the transport site (JSim code)

```
JSim v1.1 // Facilitating transporter: 2 competing solutes; includes binding steps
// Demonstrates countertransport facilitation or inhibition
import nsrunit; unit uM = 1e-6 M; unit conversion on;
math facT2 {realDomain t sec; t.min = 0; t.max = 30; t.delta = 0.1;
//PARAMETERS:
real V1 = 1 ml, //Volume 1
V2 = 1 ml, //Volume 2
Surf= 1 cm^2, //Surface area for exchange
Ttot= 1 umol/cm^2; //Transporter conc per unit surf area
real KdA1 = 10 uM, KdA2 = 10 uM, //Equilib dissociation const on each side, solute A
KdB1 = 10 uM, KdB2 = 10 uM, //Equilib dissociation const on each side, solute B
konA1 = 1 uM^(-1)*s^(-1), konA2 = 1 uM^(-1)*s^(-1), //on rates, solute A
konB1 = 1 uM^(-1)*s^(-1), konB2 = 1 uM^(-1)*s^(-1), //on rates, solute B
koffA1 = KdA1*konA1, koffA2 = KdA2*konA2, //off rates s^(-1) solute A
koffB1 = KdB1*konB1, koffB2 = KdB2*konB2, //off rates s^(-1) solute B
kT12 = 100 s^(-1), kT21 = 100 s^(-1), //free transporter flip rate 1->2 & 2->1
kTA12 = 100 s^(-1), kTA21 = 100 s^(-1), //TA flip rates
kTB12 = 100 s^(-1), kTB21 = 100 s^(-1); //TB flip rates
// STATE VARIABLES:
real A1(t) mM, A2(t) mM, B1(t) mM, B2(t) mM, // Solute concns
TA1(t) umol/cm^2, TA2(t) umol/cm^2, //TA concns
TB1(t) umol/cm^2, TB2(t) umol/cm^2, //TB concns
T1(t) umol/cm^2, T2(t) umol/cm^2; //Free transporter concns
// INITIAL CONDITIONS:
when(t=t.min) { A1 = 10; A2 = 0; B1 = 0; B2 = 0; TA1 = 0; TA2 = 0; TB1 = 0; TB2 = 0; T1 = 0.5*Ttot; }
// ODEs
A1:t = Surf*(koffA1*TA1/V1 - konA1*A1*T1/V1);
A2:t = Surf*(koffA2*TA2/V2 - konA2*A2*T2/V2);
B1:t = Surf*(koffB1*TB1/V1 - konB1*B1*T1/V1);
B2:t = Surf*(koffB2*TB2/V2 - konB2*B2*T2/V2);
T1:t = -(konA1*A1 + konB1*B1)*T1 + koffA1*TA1 + koffB1*TB1 - kT12*T1 + kT21*T2;
TA1:t = konA1*A1*T1 - koffA1*TA1 - kTA12*TA1 + kTA21*TA2;
TA2:t = konA2*A2*T2 - koffA2*TA2 + kTA12*TA1 - kTA21*TA2;
TB1:t = konB1*B1*T1 - koffB1*TB1 - kTB12*TB1 + kTB21*TB2;
TB2:t = konB2*B2*T2 - koffB2*TB2 + kTB12*TB1 - kTB21*TB2;
T2 = Ttot - TA1 - TA2 - TB1 - TB2 - T1; //Conservation of transporter.
}
```

using this code and setting the concentrations of B to zero and the other parameters as in Fig. 8-6. (This code will be used in the next section too.)

The effect of slow binding on the apparent K_d : The curvature and delay of the intercept for the curves in Fig. 8-2 is greater for small initial concentrations, $A_1(t=0)$, than for large concentrations because the relative amount held on the binding sites is less at high concentrations. There is an additional effect of slow binding, the rightward (upward) shift in the apparent K_d . Furthermore there is an increase in the steepness of the slope of the relationship between flux and concentration, mimicking an increased (but false) degree of cooperativity. In Fig. 8-7 are plotted

the fluxes in Fig. 8-2 versus the initial concentrations. The fluxes are proportional to the slopes after a pseudo-steady state has been reached. (This has to be termed “pseudo” since at substantially later times the slope diminishes; these curves are, since the flux is into a fixed volume, the first part of a near exponential curve. The steady state fluxes however do not follow

Figure 8-7: The effect of binding rate on the initial “pseudo-steady state” fluxes as a function of initial concentrations in the initial velocity experiments portrayed in Fig. 8-2. At a fast rate of binding, $10 \text{ mM}^{-1}\text{s}^{-1}$ the theoretical relationship is almost obeyed, but at slower rates the fluxes are reduced in magnitude and the half-maximal rate is shifted to higher concentrations (mimicking a lower affinity) and the slope of change of flux per increase in concentration is steeper, mimicking a degree of cooperativity when there is none.

the expected sigmoidal relationship typical of Michaelis -Menten transporters with a half-maximal rate at the K_d and a logarithmic slope of 1.0, but shift to the right giving a higher apparent K_d and, particularly in the concentration range below the apparent K_d , has a higher slope. The peak slope of the relationship for the slowest rate of binding shown, $k_{on1} = 0.2 \text{ s}^{-1}$, is equivalent to a Hill coefficient of over 2.0, when it is actually 1.0 when the binding is fast. This kind of behavior is seen also with enzymes and with even fast-binding enzymes when access to them is hindered by diffusion or membrane permeation.

8-2. Application to tracer experiments on capillary permeability

To determine the K_m and V_{max} for a transporter on the luminal surface of the endothelial cell, a series of multiple tracer indicator dilution experiments to estimate the fractional extraction of tracer at each of several background levels of nontracer S_i . Then the permeability surface area product $P_{eff}A$, and V_{max} and K_m are estimated by optimizing the fit of Eq. 8-23 to the data. An example is shown in Fig. 8-8.

This process provides estimates of K_m and V_{max} (Eqs. 8-24a and 8-24b) but these cannot be parsed to provide P' , nor can one separate the components of $T_T P_{TS}$. Another set of experiments, with $S_o > 0$ is required to estimate P' . No transient tracer experiment will separate T_T from P_{TS} —an increase in the number of transporters is as effective in increasing P_{eff} as is an increase in P_{TS} . Measurement of the concentration of the specific transporter protein by antibody labeling is one way to estimate T_T . The growing efforts to characterize the “proteome”, the nature and quantity of all cellular proteins, are beginning to provide data on intracellular enzyme concentrations; changing concentrations are taken to be evidence of genetic regulation or changing rates of proteolysis. These are a part of what Kuile and Westerhoff (2002) entitle “hierarchical regulation” of metabolic flux, to contrast it with substrate-supply-driven “metabolic regulation”.

There are potential sources of error in such experiments. The likeliest problem is that perfusing the heart with a solution of adenosine is likely to change the physiological state, reducing the vascular resistance and possibly reducing the strength of contraction. The biggest worry, however, is that having a high capillary concentration will cause a raised intracellular concentration and then influence the apparent P_{eff} by inducing countertransport facilitation or inhibition, if the relevant parameters of the system P_{TS} and P_T differ. The results in Fig. 8-8 show

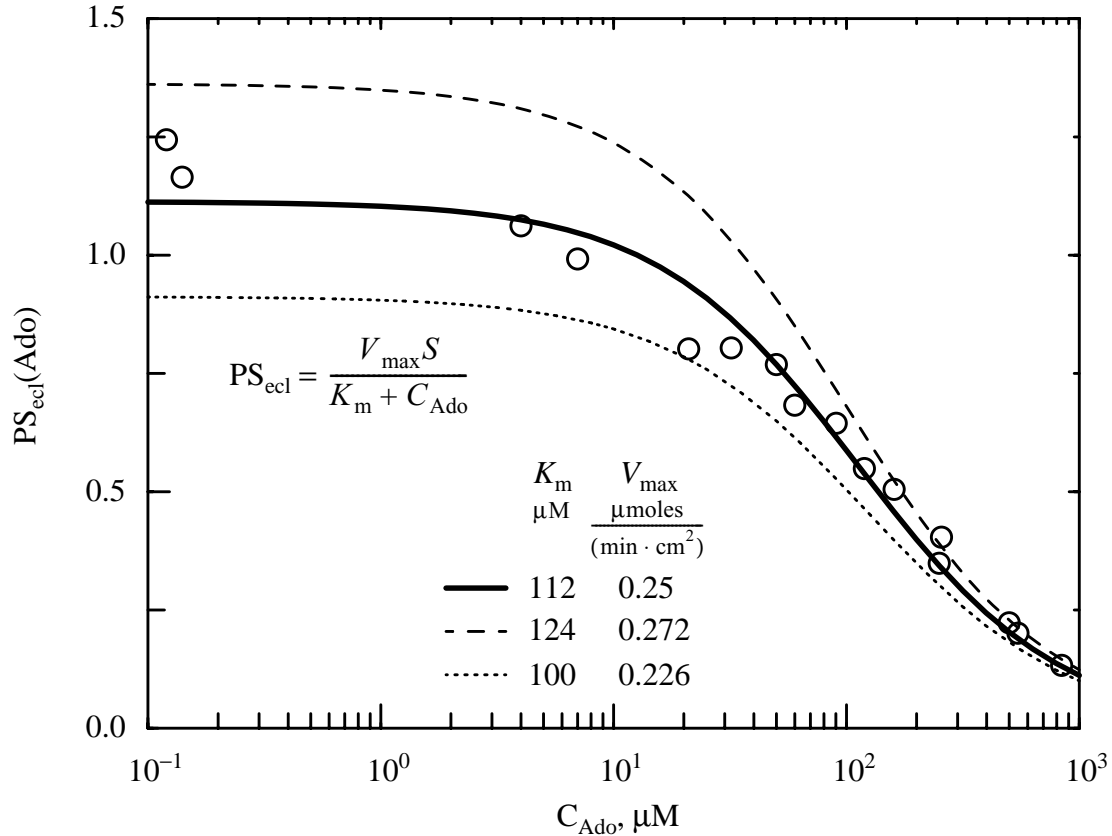


Figure 8-8: Estimated PS_{ecl} (open circles) versus venous effluent adenosine concentrations, C_{Ado} . From this, the parameters for the nucleoside transporter on the luminal surface of coronary capillary endothelial cells were estimated using nonlinear least squares optimization assuming Michaelis-Menten kinetics. This gave $K_m = 112 \pm 12 \mu M$ and $V_{max} = 0.25 \pm 0.023 \mu moles \min^{-1} cm^{-2}$ and $PS_{eclMax} = 1.12 \text{ ml } g^{-1} \min^{-1}$ for the adenosine transport, where the \pm values represent the 95% confidence limits. (Data from Krebs-Henseleit perfused guinea pig hearts. From Schwartz et al., 2000, with permission from the American Physiological Society.)

no evidence of a systematic deviation from Eq. 8-23: if there were facilitating countertransport then the data would lie above the theoretical curve at high concentrations and would fall below it if there were inhibitory countertransport. A reasonable conclusion is that $P' = 1$ for the purine nucleoside transporter in cardiac endothelial cells, as has been thought to be the case for erythrocytes (Plagemann and Wohlhueter, 1980). Cases for $P' \neq 1$ are considered next.

8-2.1. Unidirectional flux with finite trans concentration

Adding substrate to the trans side so that $S_o > 0$ changes the cis-to-trans flux, J_{io} . When $P_{TS} > P_T$, **this gives facilitating countertransport, cis-to-trans flux is raised**. (Cis is this side, trans is the other side; thus we are considering cis as inside.) The reason is that by raising S_o , converting more T_o to TS_o , more carrier is returned from trans to cis, making more transporters available on the cis side for cis-to-trans flux. This is summarized by saying that raising S_o raises γ_o in Eq. 8-18a. *Inhibitory countertransport* occurs when $P_{TS} < P_T$ so that raising S_o decreases J_{io} .

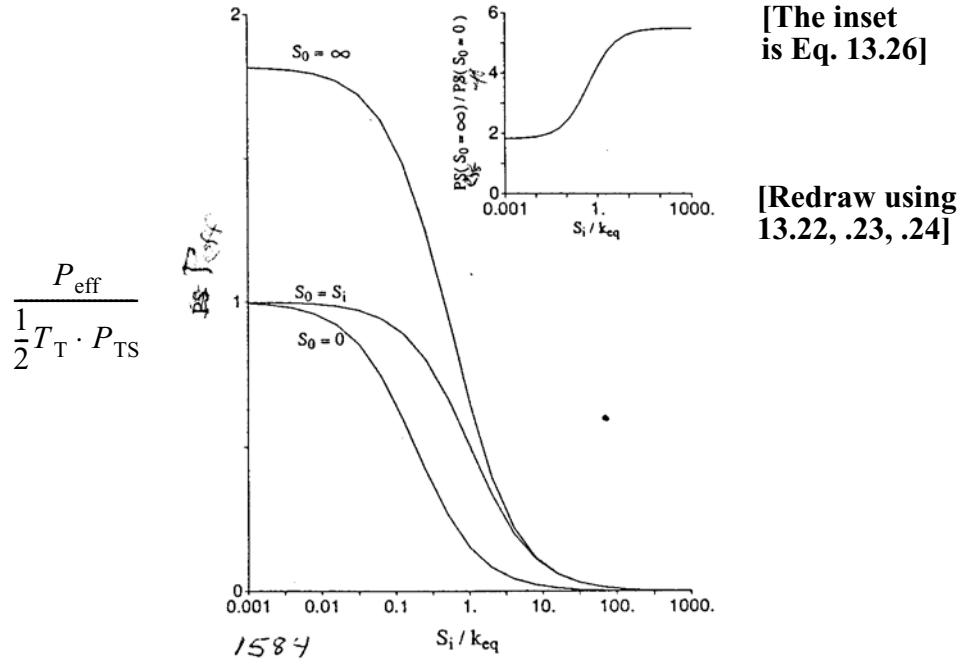


Figure 8-9: Facilitating Countertransport. With $P_{TS}/P_T = P' = 10$, the effect of raising the outside concentration S_o is to increase the P_{eff} and the unidirectional flux from inside to outside. In general $P' > 1$ gives countertransport facilitation because the transporter returns more quickly to the cis side when it is occupied by substrate from the trans side.

Figure 8-9 illustrates the effect of S_o on J_{io} : the effective membrane P_{eff} for cis to trans flux, J_{io} , as is given by Eq. 8-19, for any S_o . From this, simplified cases are derived from Eq. 8-18a:

$$\text{when } S_o = 0: P_{eff} = \frac{(1/2)T_T \cdot P_{TS}}{k_{eq} + S_i(1 + P_{TS}/P_T)/2}, \quad (8-31)$$

$$\text{when } S_o = S_i: P_{eff} = \frac{(1/2)T_T \cdot P_{TS}}{k_{eq} + S_i}, \quad (8-32)$$

$$\text{when } S_o = \infty: P_{eff} = \frac{(1/2)T_T P_{TS}}{(k_{eq}/2)(1 + 1/P') + S_i}. \quad (8-33)$$

When $P' = 1$, these all reduce to the same form:

$$P_{eff}(S_o = 0) = P_{eff}(S_o = S_i) = P_{eff}(S_o = \infty) = \frac{(1/2)T_T \cdot P_{TS}}{k_{eq} + S_i}, \quad (8-34)$$

which is the same as Eq. 8-22. In Fig. 8-9 one can see the effects of P_{TS} being greater than P_T : the apparent K_m is shifted to the left for both extreme cases, $S_o = 0$ and $S_o = \infty$. However, the relative effects of $S_o = \infty$ versus $S_o = 0$ depend on S_i :

$$\frac{P_{\text{eff}}(S_o = \infty)}{P_{\text{eff}}(S_o = 0)} = \frac{2/(1 + P') + S'_i}{\frac{2}{1 + P'} \cdot \left[\frac{1}{2} \cdot (1 + 1/P') + S'_i \right]}. \quad (8-35)$$

This is plotted in the insert in Fig. 8-9. For example, at $S'_i = 1$ and $P' = 10$ as in Fig. 8-9 (insert),

$$P_{\text{eff}}(S_o = \infty)/P_{\text{eff}}(S_o = 0) = \frac{3 + P'}{3 + 1/P'} = \frac{13}{3.1} = 4.19. \quad (8-36)$$

Note that the ratio at $S'_i = 1$ is not at the mid level between the plateaus at low S'_i and high S'_i but is a little higher; this is because the apparent K_m 's are different in the two cases:

$$K_m(S_o = 0) = 2k_{\text{eq}}/(1 + P') = 0.18 k_{\text{eq}},$$

$$K_m(S_o = \infty) = \frac{k_{\text{eq}}}{2}(1 + 1/P') = 0.55 k_{\text{eq}}.$$

8-3. Tracer transients with saturable transport

Crone (1965) showed that the effective P for tracer-labelled D-glucose in the brain was reduced by raising the blood glucose level, thereby providing direct evidence for flux mediation by a saturable transporter. The experiment was based on the principle that the injection of a bolus of tracer glucose had no effect on the apparent P_{eff} , but that the nontracer glucose level controlled P_{eff} in accord with Eqs. 8-21a and 8-21b. (Experimentally, it is therefore important that the tracer be of high specific activity so that additional nontracer content in the injectate is negligible.)

Linehan et al. (1987) introduced the “bolus sweep” technique, an experimental approach in which nontracer is injected simultaneously with nontracer mother solute in order to create a transient during which there is a changing degree of competition between nontracer and tracer. Mother solute, the same species as the tracer but with no tracer label, competes with tracer for the transporter binding site. The P_{eff} therefore changes as a function of time as shown in Fig. 8-10, where P_{eff} diminishes as the plasma concentration of nontracer rises to the peak within the capillary, and then P_{eff} rises again as the bolus washes out of the capillary. The effects on the tracer extraction are shown in Fig. 8-11. In this case the nontracer concentration was nearly zero at the earliest part of the bolus, so there was no competition from nontracer to inhibit binding of tracer to the transporter initially. When the peak bolus concentration was inside the capillary the tracer transport was about three-quarters inhibited, as shown by the reduction in the instantaneous extraction, $E(t) = 1 - h_D(t)/h_R(t)$, as the bolus sweeps past the transporter sites on the capillary endothelium.

An experiment done by Dawson et al. (1984) on the endothelial uptake of PGE_1 (prostaglandin E_1) is shown in Fig. 8-12. PGE_1 is taken up but almost none is released to return to the capillary blood, so the values of $E(t)$ again approach the maximum during the tail of the

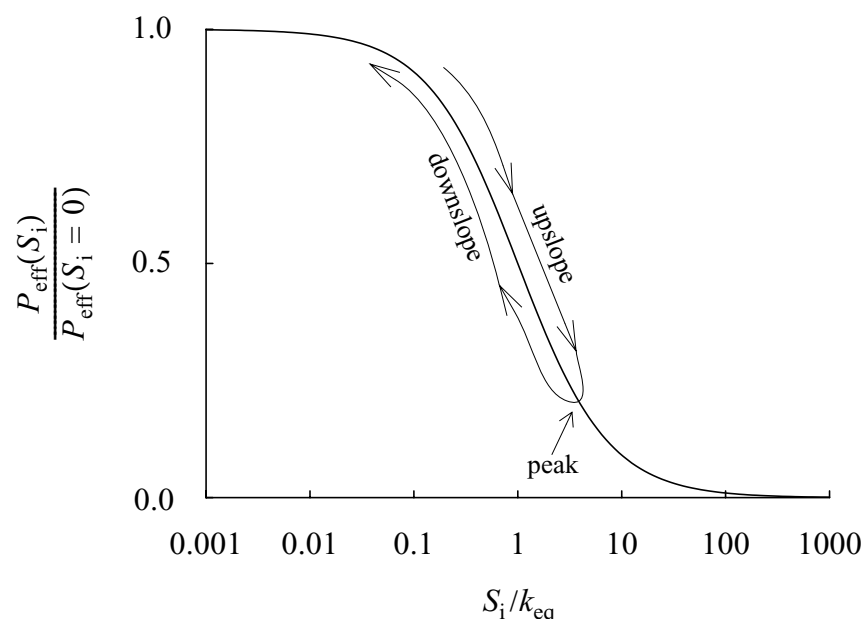


Figure 8-10: The idea of the “bolus sweep” indicator dilution experiment. Tracer and nontracer “mother” solute are injected together into the inflow to an organ in a multiple indicator dilution experiment and the outflow concentration time-curve is obtained. Mother substance competes with tracer for the binding site on the transporter in accord with its concentration; tracer concentrations are by definition negligible. The peak competition occurs at the peak of the dilution curve. (See Figure 8-11.)

washout. Note that the initial point of $E(t)$ is less than this maximum, indicating that there was some inhibition to tracer transport by the nontracer concentration in the first sample. The nontracer concentration is not plotted: while if extraction were low it would have a shape close to that of the reference tracer dextran, in this case with high tracer extraction, there will also be extraction of nontracer, about 20% at the peak concentration.

Serotonin (also known as 5-HT or hydroxytryptamine), like PGE_1 , is taken up by endothelial cells and rapidly converted to a product which doesn't leave the cell ($5\text{-HT} \rightarrow 5\text{-HIAA}$, or, in words, 5-hydroxytryptamine \rightarrow 5-hydroxyindole acetic acid). There is, however, some small return flux of serotonin which reduces $E(t)$ during the tail. (Why is the reduction in $E(t)$ more for the 10 nmol dose than for the 100 nmol dose?)

The bolus sweep experiment has one great advantage over performing a set of several indicator dilution curves at different background nontracer levels: the total mass of the solute injected in the bolus is very much less than is administered during steady infusions and the experiment is over before any physiological responses occur.

8-3.1. Additional topics for study

1. Ion pumps

0.0.1. General features: Energy transduction, influence of membrane potential, influence on action potential

0.0.2. Cardiac NaK ATPase models

2. Coupled ionic fluxes, charge-neutral exchangers

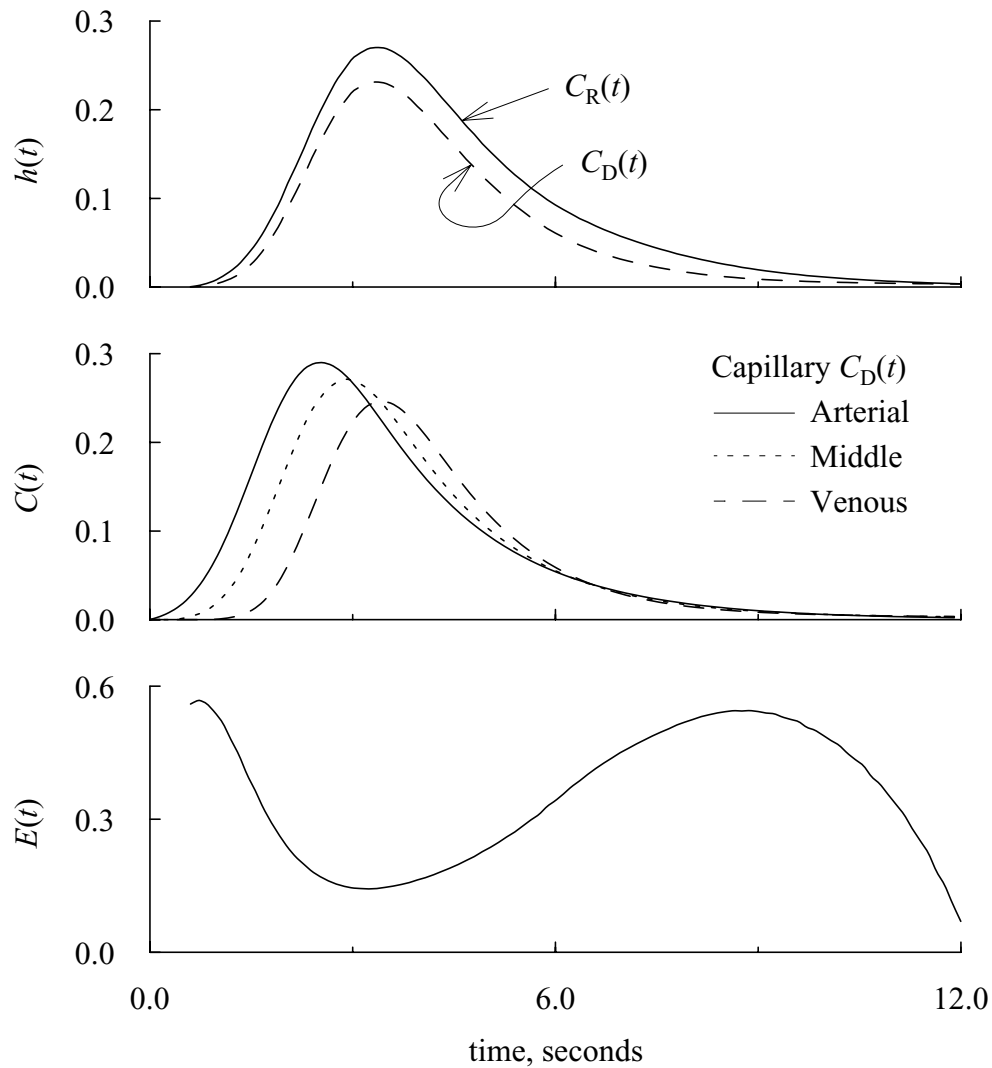


Figure 8-11: Tracer transients using the “bolus sweep” method for a solute transported across the luminal endothelial surface and consumed entirely within the endothelial cell. *Upper:* Outflow $C_R(t)$ and $C_D(t)$ normalized. *Middle:* Concentration-time curves within the capillary at upstream, midstream and downstream positions. *Lower:* The P_{eff} was reduced to about one-quarter of its zero-competition value by the peak concentration of nontracer mother solute in the bolus, as shown by the nadir in $E(t)$. Parameters were ??

8-4. Problems

1. In steady-state experiments, what is the effect of increasing or steady-state concentration in S_0 on apparent P_{eff} , etc.?
2. Compare and contrast the Barrer time-lag method for estimating the rate of diffusion through a membrane with the initial velocity method of this chapter. Consider the membrane, the transporters, binding sites, etc.

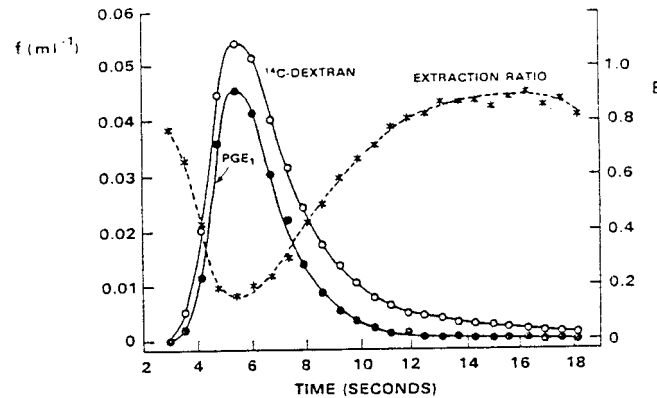


Figure 8-12: Prostaglandin E_1 , tracer outflow dilution curve from the lung. The bolus contained a near saturating dose of PGE_1 . The instantaneous extraction, $E(t)$, returns to 90% during the washout phase. From Linehan et al. [1981] with permission)

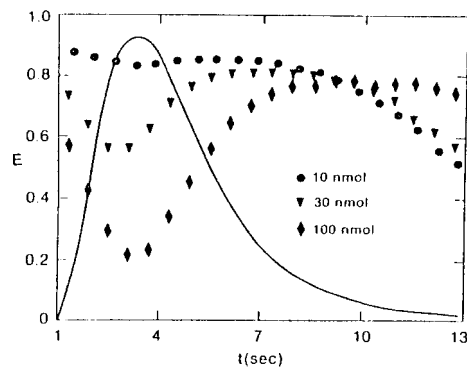


Figure 8-13: Instantaneous extraction curves $E(t)$ for tracer serotonin at three levels of background, competing dosage levels of nontracer serotonin. The continuous curve is an approximate intravascular reference curve representing those for the three separate injections. (Experiments of Rickaby, Linehan et al. 1981).

3. When there is no transporter, how would the first data points in an initial velocity experiment on a thick membrane differ from those on a thin membrane? With binding sites in the membrane? With a transporter?
4. Show the reduction of the equations for a transporter to the simple Michaelis-Menten expression for saturable transport.
5. Based on the model code for the simple transporter, write the expression for the unidirectional flux of substrate from side 2 to side 1.
6. Using the model for a transporter with a single binding site, define the conditions under which the unidirectional flux of A from V1 to V2 would be enhanced by the presence of A on side 2 ($A_2 > 0$).
7. Start with Code **facT1.proj** and load parameter set **facT1.satn3.par**: **PLOTPAGE 3**:
 Use CVODE as the solver. Run for $1e4$ seconds at $dt = 0.25$ sec.
 The conditions set up here are that $A_1(0) = 100 \cdot K_d$ for binding and $A_2(0) = 0$.
 The transport rate is low, but V2 is small so that the concentration A_2 builds up

faster than A1 is depleted.

$V1 \cdot dA1/dt$ = flux out of V1. = red curve

$V2 \cdot dA2/dt$ = flux into V2. = green curve

A2 rises from well below K_d to 60 times K_d at 10000 seconds.

Explain:

- (1) What events cause the red and the green curves to differ.
- (2) Why do they converge?
- (3) Why does $V2 \cdot dA2/dt$ have a minimum at early times and then become constant for a while.
- (4) What will be the final values of the two fluxes at $t = \infty$?
- (5) $V1 \cdot dA1/dt$ = constant from 1 to 40 seconds. How is this compatible with the changing flux, $V2 \cdot dA2/dt$?
8. Design a counter transport facilitation/inhibition experiment to see if $P' \neq 1$. (We will learn in later chapters that a convection-diffusion-permeation-reaction model, Gentex, can be used for this [in representing](#) [\[to represent -ed.\]](#) blood–tissue exchange *in vivo*.)
9. Describe and explain the conditions under which a single-site transporter which can bind either of two similar substrates competitively, A or B, can demonstrate the following behavior: Volumes on side 1 and side 2 are equal. Ignore the possibility of osmotic water flux. Solute A is initially 10 mM on side 1, zero on side 2; A1 diminishes to less than 4 mM on side 1 and A2 rises to above 6 mM on side 2, and thereafter both A1 and A2 gradually approach a concentration just below 5 mM. The solute B is available.
10. What are the determinants of the maximal countertransport facilitation? Can you develop an approximate expression for this?
11. Fig. 8-9 illustrates that substrate on the opposite side of the membrane can increase the apparent permeability. What is the effective permeability in the program [in Table 1](#)? Using the parameters [in the Table 1](#) code, calculate $P_{\text{eff}}/(0.5 T_T P_{\text{TS}})$ for an infinitely high concentration on the opposite side.

8-5. References

- Crone C. Facilitated transfer of glucose from blood into brain tissue. *J Physiol* 181: 103-113, 1965.
- Dawson CA, Linehan JH, Rickaby DA, and Roerig DL. Influence of plasma protein on the inhibitory effects of indocyanine green and bromocresol green on pulmonary prostaglandin E_1 extraction. *Br J Pharmac* 81: 449-455, 1984.
- Foster DM and Jacquez JA. An analysis of the adequacy of the asymmetric carrier model for sugar transport. *Biochim Biophys Acta* 436: 210-221, 1976.
- Klingenberg M. Membrane protein oligomeric structure and transport function. *Nature* 290: 449-454, 1981.
- Linehan JH, Dawson CA, and Wagner-Weber VM. Prostaglandin E_1 uptake by isolated cat lungs perfused with physiological salt solution. *J Appl Physiol* 50: 428-434, 1981.
- Linehan JH, Bronikowski TA, and Dawson CA. Kinetics of uptake and metabolism by endothelial cell from indicator dilution data. *Ann Biomed Eng* 15: 201-215, 1987.
- Plagemann PGW and Wohlhueter RM. Permeation of nucleosides, nucleic acid bases, and nucleotides in animal cells. *Curr Top Membr Transp* 14: 225-330, 1980.

- Rickaby DA, Linehan JH, Bronikowski TA, and Dawson CA. Kinetics of serotonin uptake in the dog lung. *J Appl Physiol* 51 (*Respirat. Environ. Exercise Physiol* 2): 405-414, 1981.
- Schwartz LM, Bukowski TR, Ploger JD, and Bassingthwaite JB. Endothelial adenosine transporter characterization in perfused guinea pig hearts. *Am J Physiol Heart Circ Physiol* 279: H1502-H1511, 2000.
- Stein WD. *The Movement of Molecules across Cell Membranes*. New York: Academic Press, 1967.
- Stein WD. *Transport and Diffusion across Cell Membranes*. Orlando, Florida: Academic Press Inc., 1986.
- Tanford C. *Physical Chemistry of Macromolecules*. New York: John Wiley & Sons, 1961.
- ter Kuile BH and Westerhoff HV. Transcriptome meets metabolome: hierarchical and metabolic regulation of the glycolytic pathway. *FEBS Lett* 500: 169-171, 2001.
- Wilbrandt W and Rosenberg T. The concept of carrier transport and its corollaries in pharmacology. *Pharmacol Rev* 13: 109-183, 1961.
- Winslow RL, Rice J, Jafri S, Marbán E, and O'Rourke B. Mechanisms of altered excitation-contraction coupling in canine tachycardia-induced heart failure, II: Model studies. *Circ Res* 84: 571-586, 1999.

NOTES:

Cases for $P' \neq 1$ are considered next.